Scan Loss Pattern Synthesis for Adaptive Array Ground Stations

WILLIAM C. BAROTT
Embry-Riddle Aeronautical University

MARY ANN INGRAM
PAUL G. STEFFES, Fellow, IEEE
Georgia Institute of Technology

We present several techniques for maximizing the contact time between low Earth orbiting satellites (LEOs) and a ground station (GS). The GS comprises an adaptive array of electronically steered space-fed lenses (SFLs). Each SFL is manufactured as a low-cost printed circuit with the result that it exhibits scanning loss. By differently orienting the boresights of the SFLs in the adaptive array, the SFL's scanning losses can be made to optimally complement the path loss of the LEO, thereby reducing the cost of the GS while maximizing the download capacity of the satellite link. The optimization, implemented with a genetic algorithm (GA), can be viewed as a kind of pattern synthesis. Such arrays will benefit Earth exploration satellite service (EESS) and telemetry applications, promising a decreased cost and increased reliability as compared with GSs consisting of a large dish antenna. We show that a network of these GSs comprising a total of fourteen small antennas can achieve an average daily data rate that is comparable with that of a single large dish antenna for the Earth Observing One (EO-1) satellite, without increasing the output power of the satellite. We also analyze the case in which the satellite transmits with a variable bit rate (VBR). Furthermore, we show that by selectively populating the focal surface of the SFL with feeds, simultaneous communications with multiple satellites can be achieved with a single GS.

Manuscript received April 11, 2007; revised August 1, 2008; released for publication March 4, 2009.

IEEE Log No. T-AES/46/3/937965.

Refereeing of this contribution was handled by M. Rice.

This work was supported by the National Aeronautics and Space Administration under Grant Number NAG5-13362.

Authors' addresses: W. C. Barott, Dept. of Electrical and Systems Engineering, Embry-Riddle Aeronautical University, Daytona Beach, FL 32114, E-mail: (barottw@erau.edu); M. A. Ingram and P. G. Steffes, Georgia Institute of Technology, School of Electrical and Computer Engineering, Atlanta, GA 30332.

I. INTRODUCTION

Earth environmental satellites and other remote sensing satellites deliver significant amounts of valuable data from their positions in low earth orbit (LEO). The data delivered by LEO satellites has many scientific, telecommunications, and military applications. The increased resolution and shortened orbital periods provided by low orbital altitudes are necessary to many of these applications, but fast orbits and ever-increasing data rates put a strain on present downlink systems.

The current ground network that supports Earth-observing LEOs has several shortcomings. Each ground station (GS) consists of one large (e.g., 10 m) dish antenna. The process of steering the antenna with the requisite precision and speed is costly. These GSs are placed in or near polar regions, such as McMurdo Station, Antarctica, and Poker Flats, Alaska, to maximize satellite contact because the LEOs have polar orbits. Simply delivering repair parts to these locations is slow and costly. Another drawback of the current network is that the GS requirement for a LEO communications system is determined by the maximum distance between the satellite and the GS. The satellites transmit constant power, so the link has an excess of up to 12 dB when the satellite is close to the GS. Finally, a large dish can track only one LEO satellite at a time. The volume and importance of the LEO data necessitates finding more economical methods of creating efficient LEO downlink systems. Also, the capability of multi-satellite communications by a single GS might enable new applications and science missions.

It is shown that it is possible to construct a network with GSs, such that each GS will receive data from these satellites by adaptively combining several small (0.75 m diameter) antennas. For the small antennas, we consider both parabolic dishes and electronically steerable space-fed lenses (SFLs) [1, 2]. This type of GS has several advantages. The SFLs are manufactured with a low-cost printed circuit technology, and the cost of the digital and RF electronics that perform the adaptive combining has dropped so low that they are being used in consumer wireless products. Electronic scanning increases reliability because of the reduction or elimination of moving parts; even partial (elevation only) electronic scanning is advantageous, because the mechanical loads are much smaller than for a big dish. The small aperture sizes of the antennas imply lower precision in steering requirements. Having many small antennas in a GS means a lower probability of catastrophic breakdown; if one antenna fails, the GS might still be able to operate at a lower data rate on the remaining antennas. The adaptive combining implies that multipath can be constructively combined and interference can be suppressed. This, together

with the low cost, implies that many of these GSs can be located in temperate, even urban, environments [3]. Finally, the multiple feed structure of the SFL enables simultaneous links with multiple satellites of the same RF band.

One disadvantage of using the low-cost SFLs as the steerable elements is that they exhibit scanning loss as the beam is steered away from boresight. This is the motivation for the study reported herein.

Adaptive combining is a very old topic [4], and it has been demonstrated for a LEO satellite GS [3]. The contributions of the present paper are threefold: 1) optimization of the orientations of the SFLs within the adaptive array to manage their scanning loss, which is a novel form of pattern synthesis; 2) analysis of variable bit rate (VBR) transmission for LEOs; and 3) an investigation of partial population of the focal surface with multiple feeds to enable multi-satellite transmission.

To the best of the authors' knowledge, no other papers have investigated this type of pattern synthesis or VBR methods to maximize the downlink capacity of an array for LEO satellite communications. Although the array described in [5] will have a dedicated subarray to increase the gain of the array near the horizon, this only will mitigate the inefficiencies and is not an analytically optimal solution. Also while others have looked at distributed arrays, i.e., the large number of small dishes (LNSD) approach in radio astronomy [6], the requirements of this application are different from those previously analyzed. In contrast to [6], the application reported here uniquely considers scan-loss synthesis and the possibility of multiple-target tracking.

The X-band downlink on the satellite Earth Observing One (EO-1) was chosen as the reference link for this analysis. This satellite is located at an altitude of 707 km and has a Sun-synchronous orbit with an inclination of 98°. When this satellite is directly over a GS, the required G/T for the GS is 10.25 dB, accounting for required margins [7].

II. THE SPACE-FED LENS ANTENNA

The primary antenna type that is used in the GS analysis is the switched-beam SFL based on the antenna being developed at the University of Colorado [1]. In the analysis, this is compared with a dish antenna with the same diameter of 0.75 m and the same efficiency. Although it is more complex than a dish antenna, the SFL is a preferred choice for a GS antenna because electronically steered antennas can reduce or eliminate the need for moving parts and mechanical tracking. Electronically steered antennas also allow for the possibility of establishing multiple downlinks using the same antennas.

The basic operation of the SFL is illustrated in Fig. 1. An incoming plane wave encounters two

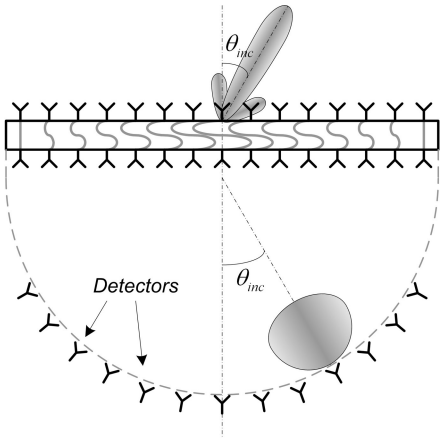

Fig. 1. Conceptual drawing of SFL.

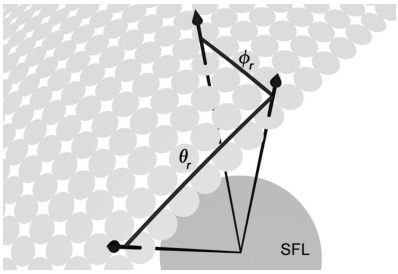

Fig. 2. Graphical representation of beam positions.

layers of radiating elements separated by fixed phase shifts (implemented as delay lines). The reradiated wave on the feed-side is focused in a small area of the focal arc; small feed elements placed in the focal arc correspond to high-gain beams radiated in known directions. A single-axis electronically steered SFL might have 32 beams placed at 2.5° increments between −38.75° and +38.75° from boresight (this small spacing was selected to reduce scalloping loss [8]). Alternatively, feeds can be placed at any location on a focal surface; an arrangement of spot beams is shown in Fig. 2, where beams are arranged in 2.5° increments along (θ_r) and perpendicular to (φ_r) a principal plane of electronic scanning. A fully populated SFL might have up to 800 feeds. The radiating elements of the SFL are patch antennas; the result is that the SFL exhibits a scan loss that follows approximately a cosine characteristic [9]. For more details about the SFL used in this analysis, including beam patterns and feed arrangements, we refer the reader to publications by the developers of the SFL, e.g., [1, 10].

We assume a system noise temperature of 148 K for the receivers consisting of the SFL and the 0.75 m dish antennas, given commercially available low-noise amplifiers (LNAs) and reasonable aperture efficiency with lossless phase shifters. We also assume that the system noise temperature does not change during scanning, e.g., from side- and back-lobes directed at the Earth. Finally, we assume that the beam of the

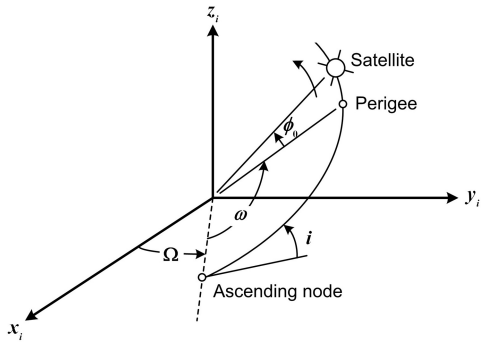

Fig. 3. Graphical representations of orbital model. From [11].

SFL that is nearest the satellite at any given time is used for communication.

III. DAILY BIT RATE DEFINITION

A. Introduction

The figure of merit used in this analysis is the daily bit rate (DBR) of the GS. The DBR represents the average number of bits that a GS can receive from the satellite in a 24-hour period.

A probabilistic approach is used to solve this problem. A probability density function (pdf) is first derived to describe the probability that the subsatellite point is within an arbitrary region on the surface of the Earth. Next, an expression is created to describe the probability that the satellite is located in a region where a communications link can be established with the GS. This expression is modified to include the effects of VBRs.

B. Orbit Descriptions

The orbits of LEO satellites can be approximated by ideal circular orbits. Two angles define the plane of the orbit: the inclination of the orbit (i) and the longitude of the ascending node (Ω). The shape of the orbit is further described by the eccentricity (one for a circular orbit), the radius of the orbit (R_S), and the argument of perigee (ω), which is set equal to 90°. The position of the satellite is described by the angle between perigee and the position of the satellite (ϕ_0) [11]. Because ϕ_0 changes at a constant rate with time, it is convenient to use $d\phi_0$ instead of dT in the calculations. A diagram of the orbit is contained in Fig. 3.

Both long-term and short-term effects cause Ω to vary as a function of time. The precession of Sun-synchronous orbits causes a change of 0.986° per day; the nodal regression caused by the rotation of the Earth causes a change of 360° per day. Due to these effects, for any random time T the angle $\Omega(T)$ is a uniformly distributed random variable between zero and 360°. Also, because $d\phi_0/dT$ is constant, the angle ϕ_0 is also a uniformly distributed random variable between zero and 360°. These two angles are uncorrelated.

C. The pdf of the Subsatellite Point

At any moment in time, the subsatellite point is uniquely defined by its latitude and longitude coordinates L_S and l_S. Because Ω is a uniformly distributed random variable, l_S is also a uniformly distributed random variable between zero and 360°. The locus of all possible subsatellite points corresponding to a given latitude L_S is a circle with a circumference given by $2\pi R_e \cos(L_S)$, where R_e is the radius of the Earth.

If L_S changes by an amount dL_S during an interval of time defined by $d\phi_0$, then the incremental area dA containing all possible subsatellite points during the interval is defined by

$$\begin{aligned} dA/d\phi_0 &= \text{abs}[dL_S/d\phi_0 \cdot \cos(L_S) \cdot 2\pi \cdot R_e^2] \\ &= \text{abs}[\sin(\phi_0) \cdot \sin(i) \cdot 2\pi \cdot R_e^2] \end{aligned} \tag{1}$$

where ϕ_0 is related to L_S by

$$\phi_0 = \arccos\left[\frac{-\cos(L_S - 90)}{\cos(i-90)}\right]. \tag{2}$$

The pdf of the satellite's location can be shown to be

$$p(L_S, l_S) = \frac{\cos(L_S)}{\pi \cdot \text{abs}[\sin(\phi_0) \cdot \sin(i) \cdot 2\pi]}. \tag{3}$$

D. Ground Station Footprint

The second step in determining the DBR of the downlink station is to define the footprint of the GS, which is the set of subsatellite points at which a transmission can occur. If the propagation loss from distance is the only variable that determines the received signal strength (E_B/N_0), then the threshold signal strength that is required for data downlink is related to an elevation angle in the local coordinates of the GS. This angle is referred to as the lowest desired elevation (LDE) angle for downlink. Transmission is possible only if the satellite is above the LDE.

The law of sines relates the LDE to the set of subsatellite points from which a signal can be received. For any latitudes L_G and L_S of the GS and subsatellite point, respectively, a value Δl_s is defined that describes the difference in longitudes for which the satellite is at the LDE [11].

The probability that a transmission can occur at any instant in time is given by the integration of (3) over the footprint of the GS:

$$P_T = \int_{-L_{\max}}^{L_{\max}} \int_{-\Delta l_s}^{\Delta l_s} p(L_S, l_S) \cdot dL_S dl_S \tag{4}$$

where $L_{\max} = \min(i, 180 - i)$. The DBR for the GS is found by $86400 \cdot P_T \cdot \mathrm{BR}$, where 86400 is the number of seconds in a 24 hr period, and BR is the bit rate of the link in bits per second.

If the communications link has several different bit rates, the aggregate DBR is given by

$$\mathrm{DBR} = 86400 \cdot \sum P_{Ti} \cdot (\mathrm{BR}_i - \mathrm{BR}_{i-1}) \tag{5}$$

where increasing indices correspond to increasing bit rates. The value of BR_0 is zero by definition.

If BR is a function of E_B/N_0, then it can be defined as a function of the latitude and longitude of the subsatellite point. The expression for the DBR will take the form of

$$\mathrm{DBR} = 86400 \cdot \int_{-i}^{i} \int_{-\Delta l_s}^{\Delta l_s} p(L_S, l_S) \cdot \mathrm{BR}(L_S, l_S) \cdot dL_S dl_S. \tag{6}$$

The highest DBR will be achieved when BR is a continuous function, and the received E_B/N_0 is always equal to the threshold value.

It is possible to find a value L_G that maximizes (6) for particular values of i and LDE. If fixed antennas are used, then the footprint of the GS can be shaped to further maximize the DBR of the network. For example, a single GS located at 64°N receives 1.7 times as much data from subsatellite points that are north of 64°N as compared with points that are south of the GS. This effect will be seen in the optimization of fixed SFL antennas.

IV. SINGLE-SATELLITE COMMUNICATIONS

A. Pattern Synthesis Approach

When the LEO satellite EO-1 is near the horizon, the path loss on the link is 12 dB higher than when the satellite is at zenith. If mechanically steered identical dish antennas are used in the GS, the required gain of the array is determined by the path loss at the LDE, and the array will have more gain at higher elevation angles than is necessary for demodulation. If the array consists of antennas that have fixed orientations and significant scan loss, optimization of the boresight directions of the antennas can make the received E_B/N_0 independent of the elevation angle of the satellite. This boresight direction optimization can be viewed as a novel kind of pattern synthesis.

The term is recently associated with numerical optimization methods, such as genetic algorithms (GAs), in sidelobe optimization [12, 13] and antenna design [14, 15]. The latter was applied to the propagation loss matched antenna (PLMA) in development at the Georgia Institute of Technology [16]; in the PLMA is an array of identically oriented fixed antennas for downlink from LEO satellites.

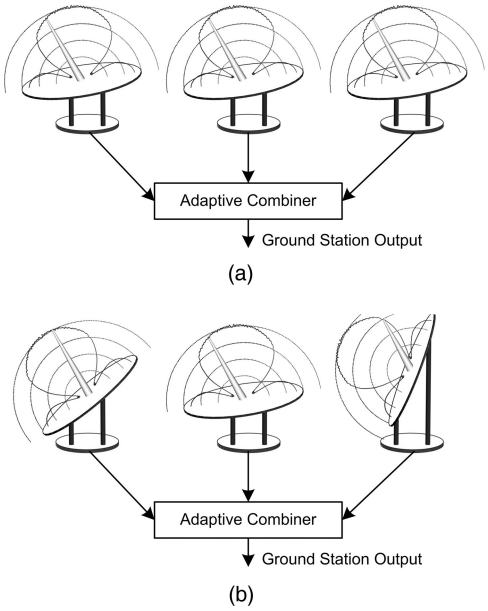

Fig. 4. Possible GS configurations using SFL. SFLs in (a) are all tilted to same angle. SFLs in (b) are tilted at different angles. Scan loss behavior is overlaid with 10 dB intervals.

The difference between traditional pattern synthesis and what is reported here is that traditional synthesis assumes an element pattern for an antenna with a fixed orientation and follows with an optimization of the complex weights or locations of the elements to create a specific array radiation pattern, usually with certain sidelobe characteristics [4]. For the synthesis considered in this paper, the "element pattern" is the peak mainlobe gain of the SFL as a function of its steering angle. The peak mainlobe gain of the SFL is the pattern of the patch elements that compose the SFL times the array gain of the SFL. There is no consideration of sidelobes here because we assume that each SFL mainlobe is always steered in the direction of the satellite. Finally, instead of varying the combining weights or the locations of the elements in traditional pattern synthesis, here we vary the boresight direction of each SFL, which amounts to a rotation of the SFL "element pattern." Fig. 4(a) shows three antennas, electronically steered in elevation and mechanically steered in azimuth (the small disk at the base of each antenna represents a turntable). The narrow spikes in the drawing represent mainlobes. The large lobes in each drawing represent the mainlobe gain as a function of steering angle, in other words, the scanning loss. When several such electronically steered antennas are used in a GS, the boresight directions of the antennas can be different. The boresight directions are optimized so that the adaptive combination of the antenna outputs yields the highest possible DBR; in effect, the scan loss is made to complement the path loss. Fig. 4(b) shows a

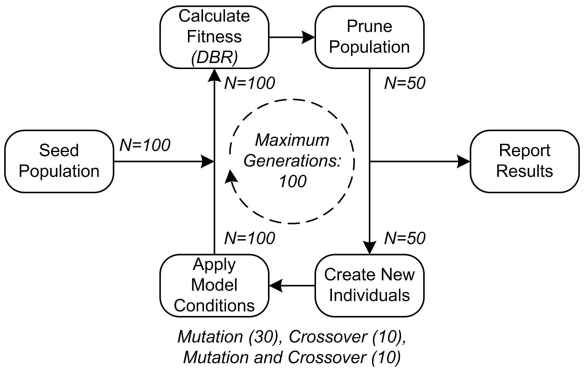

Fig. 5. Iterative process flow of GA used in this study. Crossover spawning spliced parent genes at a random position. Mutation spawning altered orientation genes by up to 15 deg.

possible outcome of the optimization. The boresights of the three antennas are oriented differently. While the mainlobes are steered in the same direction, each antenna has a different value of scan loss.

A GA was selected as the optimization method for the antenna orientations. A GA is a numerical optimization method that resembles the processes of evolutionary biology. During each generation, or iteration of the algorithm, the population of solutions evolves toward the best global solution; the process follows the order shown in Fig. 5. The description in [17] provides a comprehensive summary of GAs and their uses in electromagnetic problems.

This scanning loss can be described by the function $G(\psi)$ where ψ is the elevation angle off-boresight, such that $G(0) = 1$. If the peak power gain of the SFL in the boresight direction is given by a constant A, then the power gain of the SFL when scanned to the angle ψ is $AG(\psi)$. The path loss between the GS and the satellite can be defined as $L_P(\theta)$, where θ is the elevation angle of the satellite. In the absence of interference, the array gain can be expressed according to maximal ratio combining (MRC) [18]. MRC yields an optimal post-combiner signal-to-noise ratio (SNR) that is the sum of the input SNRs, or, equivalently, the power gain of an array using MRC is the sum of the individual antenna power gains in the direction of the satellite. MRC assumes that precombining phase adjustments are chosen to offset for inter-element relative phases caused by the physical separations between SFLs and the different phase responses of the SFL patterns in the direction of the satellite. If there are N SFLs and no other loss mechanisms, then the part of the link gain that depends only on the path loss and the SFL mainlobe gains can be expressed by

$$G_L(\theta) = \left[A \cdot \sum_{n=1}^{N} G(\theta - \psi_n)\right] \Big/ L_p(\theta) \qquad (7)$$

where ψ_n is the boresight direction in elevation of the nth SFL. The GA optimizes the values of the

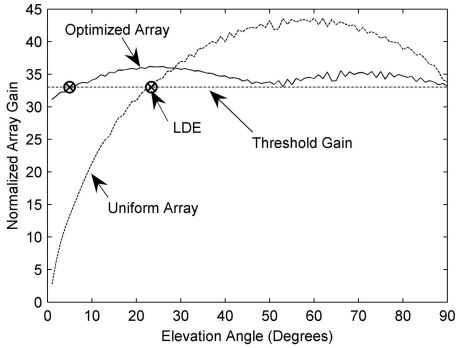

Fig. 6. Normalized link gain of optimized SFL array as function of elevation angle.

$\{\psi_n\}$ to minimize the first elevation angle at which the received E_B/N_0 drops below the threshold value. Optimizing $\{\psi_n\}$ is equivalent to optimizing the physical orientation of the antennas within the array. The positions of the antennas within the array are also important, and if improperly chosen will result in the presence of grating lobes (aliases) in the array factor. These aliases are detrimental to imaging and cochannel nulling, but are unimportant to MRC, which assumes no interference. Grating lobes can be removed from the array factor pattern using similar optimization techniques (e.g., [12, 13]) without impacting the current analysis.

B. Single Ground Station Results

Fig. 6 contains plots of $G_L(\theta)L_P(90°)$ for two cases. The optimized design has an LDE of 5° with eight antennas; despite the slightly lower gain and high scan loss of the SFL, this is only one more than is required for an array of 0.75 m dishes assuming equal antenna efficiencies. The uniform array in which all boresights are pointed at an elevation of 50° has an LDE of only 23° and an excess gain of more than 10 dB at some angles. The DBR of the optimized array is almost four times that of the uniform array, because the satellite moves much more slowly through low elevation angles than it does at high elevation angles. Additionally, a uniformly oriented array requires more than 90 antennas for an LDE of 5°.

Fig. 7 contains plots of the DBR per antenna for similar GSs located at the latitude of Seattle, Washington (47.6°N), corresponding to the 105 Mbit/s downlink on EO-1, The x axis represents the number of antennas at the GSs; a higher number corresponds to a lower LDE and a higher total DBR. With the exception of the nonoptimized SFL array, the DBR per antenna increases for each array as the number of antennas is increased. Doubling the number of antennas more than doubles the probability that a signal can be received because the area of the footprint more than doubles, and the footprint grows toward the polar regions where the satellite is more likely to be.

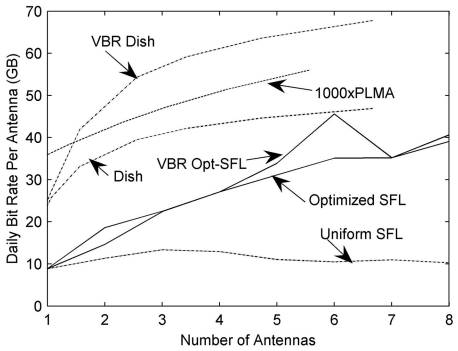

Fig. 7. DBR per antenna as function of total number of antennas at GS, located at 47.6°N. Individual plots are annotated.

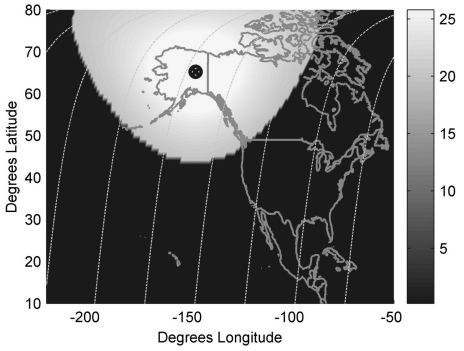

Fig. 8. Received signal strength as function of subsatellite point for single downlink station located at Poker Flats site.

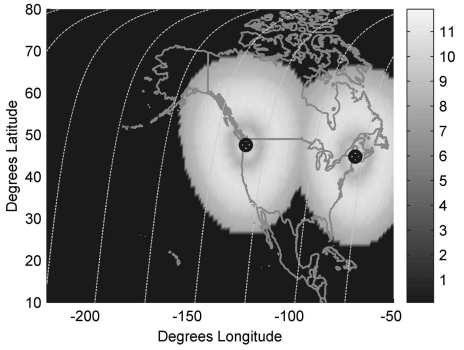

Fig. 9. Received signal strength as function of subsatellite point for two downlink stations consisting of SFLs, located in Maine and Washington. Shading scale range is different than Fig. 8 to enhance readability.

VBR transmission is an alternative approach to the excess link gain problem. Ideally, as the path loss varies in the course of a pass, the satellite would change the modulation level (BPSK, QPSK, etc.) so that the bit rate would change, but the received bit energy-to-noise ratio E_B/N_0 would be constant. Practically, only a few modulation levels would be employed. In the two VBR cases in Fig. 7, the bit rates are 105 Mbit/s and 210 Mbit/s. Including the higher bit rate significantly increases the DBR of the dish antenna GSs because the dish antenna stations have an excess gain of up to 12 dB at some angles. The maximum improvement relative to the constant modulation case is a factor of 2.7 when an ideal and continuously VBR method is used. On the other hand, combining VBR with boresight optimization (VBR opt-SFL) offers only a slight improvement over constant modulation with boresight optimization (optimized SLF or opt-SFL) because the SFL array is optimized so the received signal strength does not change significantly as the satellite gets closer to the GS.

C. Network Simulations

The orbital descriptions and results of GS optimization were used to develop a numerical network simulator. This generated network data for various configurations of GSs at various locations. The simulator switched the transmission between GSs by selecting the GS with the highest E_B/N_0 for transmission at a given instant in time. The DBR was found by averaging the integrated capacity of many orbits and multiplying this capacity by the number of orbits per day.

The design goal for these networks was to meet or exceed the DBR of a single 11 m dish antenna downlink station, for EO-1, located at the Poker Flats facility in Alaska. For the purpose of this analysis the minimum LDE is restricted to 5° above the horizon. In all cases, the threshold SNR for demodulation is taken as 6.5 dB.

Fig. 8 shows the received E_B/N_0 as a function of the position of the subsatellite point for the reference case of a single 11 m dish antenna at Poker Flats. The boundary of the coverage area for this antenna is defined by the LDE rather than the minimum signal strength. Fig. 9 shows, with an enhanced scale, the signal strength for a network of two GSs, each comprising 8 SFLs, with one GS in Seattle, WA, and one in Bangor, ME. We observe that the signal strength variation in Fig. 9 is more nearly constant than in Fig. 8, which is consistent with the results in Fig. 6.

Table I contains DBR results for a number of different network configurations. The variables in the network include the number of GSs, the position of the GSs, the number of antennas per GS, and the data rate. Both fixed and VBR models are considered. All but the last assume 0.75 m dish antennas. The last one, which corresponds to Fig. 9 and which uses SFLs with optimized boresight directions, achieves a DBR approximately equal to that of the Poker Flats antenna. We observe that several networks produce DBRs comparable with the Poker Flats facility; among these is the case that uses a constant 50 Mbit/s data rate and a total of only thirteen 0.75 m dish antennas. This somewhat surprising result happens because the decreased data rate lowers the minimum elevation for demodulation where the satellite's rate of elevation change is very slow.

TABLE I
Network Configurations and Performance

TX Rate (Mbit/s)	Network Configuration	Total Antennas	DBR (GBit)
105	11 m (PF)—Reference	1	585
50	7×2 (S, B)	14	279
50	3×2 (S, B)	6	270
50, 100	3×2 (S, B)	6	395
50, 100, 200	3×2 (S, B)	6	497
50, 100	3×3 (S, B, T)	9	501
50, 100, 200	3×3 (S, B, T)	9	642
105	3×2 (S, B)	6	246
105	7×2 (S, B)	14	587
105	5×3 (C, H, DC)	15	545
105	5×2 (H, DC) 6×1 (C)	16	578
50	3×4 (H, S, B, T)	12	427
50	3×3 (S, B, H) 4×1 (PF)	13	594
105	8 SFL $\times 2$ (S, B)	16	587

Note: Network configuration is: number of antennas per station $\times$ number of stations (station codes). Station codes include: Bangor, Maine (B), Stockton, California (C), Washington, D.C. (DC), Honolulu, Hawaii (H), Poker Flats, Alaska (PF), Seattle, Washington (S), and Corpus Christi, Texas (T).

V. MULTI-SATELLITE COMMUNICATIONS

The multiple-feed structure of the SFL and other antennas, such as the Luneburg lens [19, 20], enables simultaneous communications with multiple, spatially separated satellites. Also, since there are several SFLs in a GS, different SFLs could communicate with different satellites. As the satellites, including those transmitting in the same band, travel in "trains," there is a significant opportunity for multi-satellite communications. Within a single SFL, this is accomplished using an N-to-M switch, where N is the number of feeds and M is the number of satellites to be tracked. M radio chains per SFL are required for reception of the M satellite transmissions. Because the radio chains have a significant cost, there is a motivation to investigate if multiple satellite links can each have connect times similar to the single-satellite case, with some number of feeds less than the up to 800 (at 2.5° spacing) required to fully populate the focal surface.

Although at least 1 min separations within the train are considered, it is assumed that multi-user detection receiver signal processing [21] would be required when the satellite transmissions are cochannel, because of the overlap of beam patterns associated with different feeds. In the analysis below, any degradation to the received E_B/N_0 that would result from imperfect cochannel interference suppression are ignored. Detailed modeling of these degradations and how they affect network performance is left as a subject of future research.

This investigation has three parts. For the first part, a fully populated focal surface (i.e., full electronic scanning) is assumed, and the relative frequencies of feed excitation are presented. Two satellites in a train are separated by one or two minutes, and the mechanically steered azimuth angle of the SFL was chosen to be halfway between the azimuth coordinates of the two satellites. The relative frequencies tell us what subset of potential feed locations can provide most of the connect time. In the other two parts, two partial feed population design strategies are considered. In the first strategy, a mix of mechanical and electronic scanning is considered, and the boresight angles of the antennas are optimized to provide maximum contact time for a given pass of a train. In the second strategy, no mechanical scanning is assumed, and the object of the optimization is maximization of the DBR.

A. Relative Frequency of Beam Excitation

One method of analysis is to assume a grid of possible beam locations as shown in Fig. 2. For a particular satellite separation and tilt angle, it is possible to calculate how often each feed location is used and thus how many feeds are necessary for each antenna. Fig. 10 contains beam relative frequency intensity plots for antennas with tilt angles (θ_t) of 5° and 60° for satellite separations of 1 and 2 min. These plots do not depend significantly on the latitude of the GS. The origin of each plot represents the boresight pointing angle; the x and y axes represent the beam positions in φ_r and θ_r, respectively. We observe that the azimuth distribution of excited feeds broadens with increasing tilt angle and roughly doubles with the doubling of satellite separation. Many feeds are never excited, and therefore are not needed for these satellite separations. The feeds at the highest values of azimuthal separation are seldom excited.

Next, we consider how much connect time with the satellites is lost if we remove the least excited feeds. This is referred to later as the "close track" approach. Fig. 11 shows the percentage of the maximum connect time as contours plotted against tilt angle (θ_t) and the number of feeds for a 1 min separation (left) and a 2 min separation (right). It is seen from the figure that required contact time of 90% of the maximum time implies between 75 and 200 feeds for the each SFL antenna.

B. Per-Train Optimization with Mechanical and Electronic Scanning

The method of Section IV, which optimizes the fixed boresight angles assuming electronic elevation scanning and mechanical azimuth scanning, is insufficient for multi-satellite tracking from a single GS. This is because the satellite train and the GS are not contained in a single plane.

One alternative arrangement is to add mechanical axes to the antennas, add more feeds, and optimize

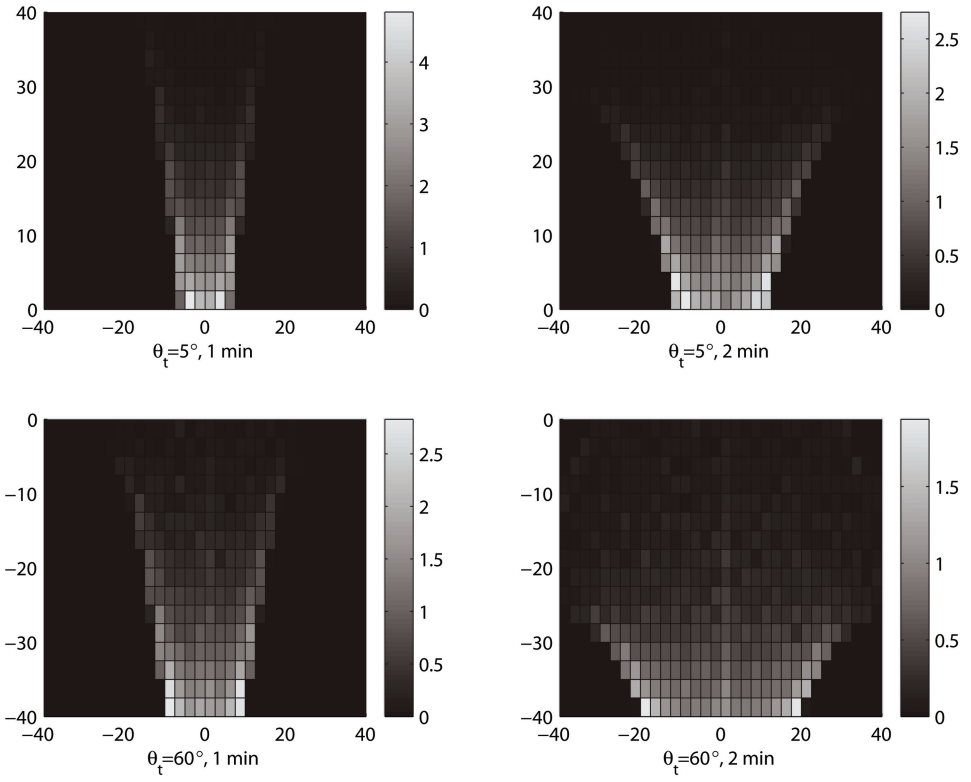

Fig. 10. Density of beam stimulation for different SFL tilt angles and different satellite separation times. Plotted for percentage of total time for single beam for intensity scale. x axis represents off-boresight azimuthal angle; y axis represents off-boresight elevation angle.

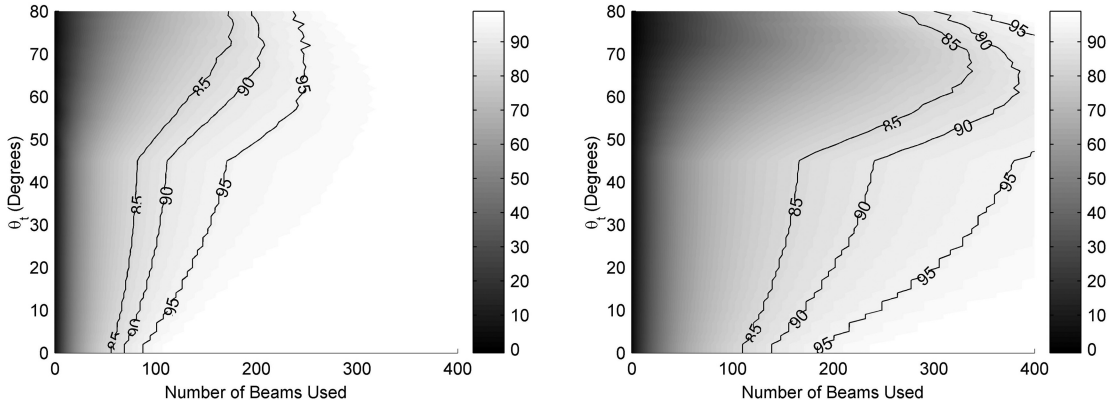

Fig. 11. Percentage of maximum contact time achieved as function of SFL tilt angle and number of feeds used in SFL. Plotted for 1 min satellite separation (left) and 2 min separation (right).

the antennas' boresights to maximize contact time along an orbital plane as projected into local coordinates. This approach is referred to later as the "Path Track" method. For this optimization, the figure of merit of the algorithm is defined as the ratio of the contact time with a single satellite to the maximum contact time for a single pass. The algorithm calculates this value by dividing the pass into many small time increments; for each time increment, the algorithm determines if a communications link can be established. The total number of points where a link can be established divided by the total number of points overall is the ratio of contact time for a single pass, which is defined as all parts of the pass that are higher than 5 deg elevation. The algorithm optimizes the mechanical orientations of the antennas so that the contact time with the satellite on during that particular pass is maximized.

If the scan ranges θ_r and φ_r are equal, then it is sufficient to mechanically steer these antennas in two angles (azimuth and elevation). If the electronic scan ranges are not equal, then it is necessary to add a third mechanical axis to control the axial roll of the antenna. If the satellites in the train are in the same orbit, then these mechanical axes must be constantly attended. On the other hand, if the satellites in the train share the same ground track, these mechanical

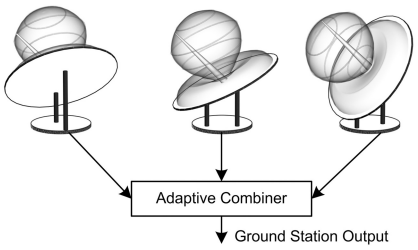

Fig. 12. Possible GS configurations using SFL. SFL focal surfaces are assumed to be fully populated, and each SFL is tilted to different fixed azimuth and elevation coordinate.

axes can be set prior to a pass event and then locked until the pass is completed.

The number of antennas that are required for this optimization process to achieve high bit capacity values depends on several factors, including the population of feeds in the aperture and the particular path that the satellites take through the sky. If fully populated SFLs are used, then 24 antennas provide an average contact time, and thus a DBR, of 95/the maximum value for a single satellite, considering all possible paths. Limiting the scanning range of the SFL to within 15° of the principal plane eliminates more than half of the required feeds but reduces the contact time to just 85% of the maximum value, again averaging the contact times of all possible paths. The contact time for an individual pass depends on the maximum elevation angle of the pass. For example, for the case limiting the scan range to 15° off the principal plane, the optimized contact time is almost 96% for an overhead pass, but is only 81% for passes that peak at 30° above the horizon.

C. Electronic-Only Scanning

If the cost of additional feeds for the SFL is low, moving parts can be eliminated while allowing simultaneous multi-beaming outside of a single satellite train. In this case, we can modify the model to optimize azimuth and elevation tilt angles for an array of fixed antennas, and we assume a fully populated aperture as shown in Fig. 12. This approach is referred to later as the "Full Sky" method. The new optimization is designed to maximize the DBR of a constant data rate link according to the method of Section IIIC.

Arrays of this type using 64 antennas achieve high per-satellite DBRs that are 93% of the dish-equivalent DBR goal of this optimization. This implies a high number of feeds, but the benefit is the complete elimination of moving parts and the ability to form many simultaneous beams to arbitrary coordinates.

Footprint plots for GSs located at 34°N and 64°N using 32 antennas are shown in Fig. 13. Reducing the number of antennas by a factor of two (from 64 to 32) reduces the DBR to 48.8% of the original value. We use the 32-antenna case in this plot to emphasize the pdf dependence of this analysis. The higher latitude optimization shows the benefit of optimizing the array based on the probability integral (6). Because there is only a small probability gradient at lower latitudes, the footprint displays no clear structure, but the footprint from the higher latitude displays a clear structure that is arranged to obtain a high contact time from the high-probability regions near the poles. Two "eyes" or holes in the coverage region, are observed in each of these plots. These correspond to look-angles near zenith, and are a result of the optimization goal and also of the scanning-loss of the SFL. An incremental solid angle in local coordinates (representing the effective scanning capabilities of a SFL) contributes to a larger geographic coverage area for SFL boresight elevations near the horizon, compared with boresight elevations near zenith. To "fill-in" these eyes would require repositioning one (or more) of the antennas in the array, resulting in a net reduction in coverage area and thus loss in capacity.

Table II contains the multi-satellite DBR results for a number of different GS configurations located at Poker Flats, Alaska. The fifth and sixth columns of this table list the per-satellite DBR and the number

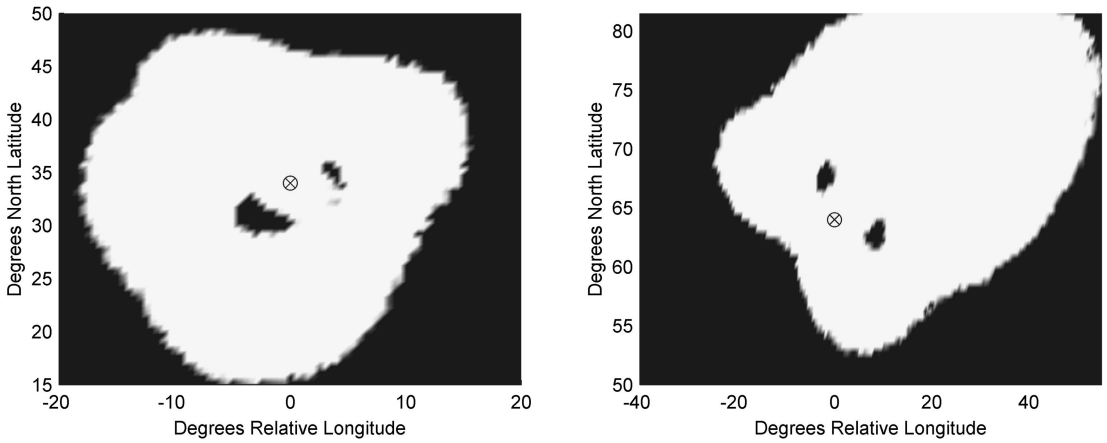

Fig. 13. GS footprint for GS located at 34°N (left) and 64°N (right) using 32 fixed SFLs. GS position is marked for reference.

TABLE II
Multi-Satellite Ground Station Optimization and Performance

Model	Note	Total Antennas	Total Feeds (xE3)	DBR/Sat (GBits)	No. of Satellites
Reference	11 m dish at Poker Flats	1	—	585	1
Single	Standard, one satellite	8	0.14	585	1
Close Track*	1 min separation	10	1.0	526	2
Close Track*	2 min separation	20	3.9	526	2
Path Track	15 deg off plane	24	9.2	498	Up to $M^{\dagger}$
Path Track	Fully populated aperture	24	19.2	560	Up to $M^{\dagger}$
Full Sky	Fully populated aperture	32	16.4	266	Up to $M^{\dagger}$
Full Sky	Fully populated aperture	64	31.6	545	Up to $M^{\dagger}$
Full Sky	Half populated aperture	64	17.8	450	Up to $M^{\dagger}$

Note: DBR analysis based on GSs located at 64°N, at the Poker Flats facility in Alaska.

Feeds based on the definition of a fully populated aperture extending to 40° from broadside. Reducing this scan angle will increase the number of antennas but can reduce the total number of required feeds.

*Close track antennas and feeds estimated based on scan loss behavior of the SFL and the beam density plots from Fig. 12.

†M is the maximum number of satellites in the field of view of the GS.

of satellites, respectively. This means, for example, that either of the GS designs based on the close-track method (rows three and four) have a total DBR of 1.052 terabits.

The row of this table with model type "single" describes a GS with the same SFL configuration as that listed in the last row of Table I, but since the GS in Table II is located at a high latitude, only one station is required to provide a high DBR as opposed to the two that are required in Table I. Under the assumptions in Section II, the GS would have $8 \times 32 = 256$ feeds, yet only 140 feeds are indicated in Table II. This is because most of the antennas in this configuration are pointed to tilt angles near the horizon, and feeds that would form beams below the horizon are not included as they provide no benefit to the array.

The close-track array can provide high data rates to two satellites that are in the same orbit, but these satellites must be located very close to each other or the number of required feeds becomes large. Approximately 3900 feeds are required if the satellites are 2 min apart, as compared with 1000 feeds if the satellites are 1 min apart. The array in this method mechanically steers to the azimuth angle between the two satellites and then uses electronic steering to form beams to the satellites. As the satellites become further apart, the utilized beams move off the principal plane of the SFL (the azimuthal scan angle increases). This causes additional scan-loss compared with the single-satellite case, and the effectiveness of each SFL decreases, requiring a greater total number of antennas (and thus feeds). This additional scan-loss makes this method unviable for all but very close satellite separations.

Much wider satellite separations are accommodated using more feeds by the path track method. This method dynamically organizes the array so that a communications link can be established from any point on an orbital plane, and requires many feeds (almost 10,000) but can establish as many communications links as there are satellites visible that occupy that orbital plane.

A limiting factor in the maximum number of satellites that could be tracked is the minimum angular separation (from the GS point of view) between cochannel satellites. This separation depends on the performance of the multi-user detection (MUD) algorithm [19], which is beyond the scope of this paper; however, separations approximately equal to an SFL beamwidth, e.g., 5 deg, should provide sufficient cochannel interference suppression by the SFL sidelobes to enable a MUD algorithm to perform adequately.

It is noted that because the scan loss of the SFL is very large at scanning angles far from boresight, it is possible to use fewer than the maximum number of feeds per SFL, thus limiting the field of view (FOV) of each SFL. However, feeds with a very high scanning loss do not contribute significantly to the DBR of the GS as compared with feeds with very little scanning loss. The last two lines of Table II illustrate this point: A full-sky optimized array using 31.6E3 feeds has a DBR/satellite of 545 Gbits/day. Reducing the number of feeds to 17.8E3 (56% of the original value) results in a DBR/satellite of 450 Gbits/day (82% of the original value).

The path track and full sky arrays require a large number of antennas and feeds as compared with a single azimuth turntable SFL design, with feeds numbering in the tens of thousands as opposed to 140. The benefit of these arrays is that they allow multiple beam forming to many satellites simultaneously: the path track array can form beams to satellites within the same train, and the full sky array can form beams to any satellites within the FOV of the GS.

The number of satellites M is currently small, with satellite trains consisting of fewer than 10 simultaneously visible satellites. EO-1 is in a Sun-synchronous group consisting of three other satellites which cross the equator at about 10AM local standard time (Landsat-7, Terra, and SAC-C). Following a similar orbit, the afternoon train ("A Train") consists of five satellites (Aqua, Cloudsat, Calipso, Parasol, and Aura), with additional satellites (OCO-2 and Glory) anticipated [22]. The number

of satellites visible in the FOV of the full-sky array is similarly small.

If the number of feeds is the only metric of cost, then it might not be economically viable to use the multi-satellite arrays. Rather, it might be more cost effective to simply duplicate the single satellite array for as many satellites as need to be simultaneously tracked. However, if the number of antennas (as opposed to the number of feeds) is significant in the cost calculation of the array, then it is noted that the path track array requires only three times as many antennas as a single satellite array but can service many satellites.

VI. CONCLUSIONS

This paper has considered the design of GSs that use small multi-beaming antennas for LEO satellite communications. These GSs will use adaptive multi-beaming techniques to form beams to one or more target satellites. Employing VBRs on the communications link can maximize the amount of data that is downloaded to a particular GS, but requires more complexity on the satellite. Alternatively, we have shown that employing scan loss pattern synthesis can provide nearly the same improvement in data capacity of the link without requiring changes to the satellites. We have proposed several optimization models and results using the SFL antenna as the fundamental antenna of the GS. We have also shown that when transitioning from costly large dish antennas to smaller inexpensive GSs, it is feasible to increase the number of GSs and move them to lower latitude urban accessible locations. Such a distributed network has an acceptable level of increased complexity, and can maintain current DBRs.

We have also shown that the bit rate BR of the channel should be maximized only insofar as it does not increase the LDE of the GSs; otherwise, increasing BR can actually lower the DBR of the network by the same principle.

ACKNOWLEDGMENT

The authors thank John Langley of the Saquish Group for his role in analyzing the 0.75 m antenna downlink stations.

REFERENCES

[1] Popovic, D. and Popovic, Z.
Multibeam antennas with polarization and angle diversity.
IEEE Transactions on Antennas and Propagation (Special Issue on Wireless Communications), May 2002, 651–657.

[2] Zhou, Y., Rondineau, S., Popovic, D., Sayeed, A., and Popovic, Z.
Virtual channel space-time processing with dual-polarization discrete lens antenna arrays.
IEEE Transactions on Antennas and Propagation, **53**, 8 Pt. 1 (Aug. 2005), 2444–2455.

[3] Ingram, M. A., Romanofsky, R., Lee, R. Q., Miranda, F., Popovic, Z., Langley, J., Barott, W. C., Ahmed, M. U., and Mandl, D.
Optimizing satellite communications with adaptive and phased array antennas.
Presented at the 2004 Earth Science Technology Conference, Palo Alto, CA, June 22–24, 2004.

[4] Van Trees, H. L.
Detection, Estimation, and Modulation Theory, Part IV: Optimum Array Processing.
Hoboken, NJ: Wiley, 2002.

[5] Tomasic, B., Turtle, J., Liu, S., Schmier, R., Bharj, S., and Oleski, P.
The geodesic dome phased array antenna for satellite control and communication—Subarray design, development, and demonstration.
Presented at the 2003 IEEE International Symposium, Oct. 14–17, 2003, 411–416.

[6] DeBoer, D. R. and Bock, D.
The Allen telescope array: Splitting the aperture.
IEEE Microwave Magazine, **5**, 2 (June 2004), 46–53.

[7] NASA
Radio Frequency Interface Control Document (RFICD) Between the Earth Orbiter (EO)-1 Spacecraft and the Spaceflight Tracking and Data Network (STDN).
National Aeronautics and Space Administration, Goddard Space Flight Center, Nov. 2000.

[8] Li, K-H., Ingram, M. A., and Rausch, E. O.
Multibeam antennas for indoor wireless communications.
IEEE Transactions on Communications, **50**, 2 (Feb. 2002), 192–194.

[9] Mailloux, R. J.
Phased Array Antenna Handbook.
Norwood, MA: Artech House, 1993.

[10] Lee, R. Q., Popovic, Z., Rondineau, S., and Miranda, F. A.
Steerable space fed lens array for low-cost adaptive ground station applications.
In *Proceedings of the International Symposium on Antennas and Propagation*, June 2007, 2136–2139.

[11] Pratt, T. and Bostian, C. W.
Satellite Communications.
Hoboken, NJ: Wiley, 1986, 11–30.

[12] Bray, M. G., Werner, D. H., Boeringer, D. W., and Machuga, D. W.
Optimization of thinned aperiodic linear phased arrays using genetic algorithms to reduce grating lobes during scanning.
IEEE Transactions on Antennas and Propagation, **50** (Dec. 2002), 1732–1742.

[13] Haupt, R. L.
Thinned arrays using genetic algorithms.
IEEE Transactions on Antennas and Propagation, **42** (July 1994), 993–999.

[14] Altshuler, E. E.
Electrically small self-resonant wire antennas optimized using a genetic algorithm.
IEEE Transactions on Antennas and Propagation, **50** (Mar. 2002), 297–300.

[15] Linden, D. S.
The twisted Yagi antenna optimized with a genetic algorithm: A potential alternative to the helix.
Presented at the 2003 IEEE Antennas and Propagation Society's International Symposium, Columbus, OH, June 22–27, 2003, vol. 1, 153–156.

[16] Barott, W. C. and Steffes, P. G.
Antenna and topology choices for a large N array for LEO satellite downlink.
Presented at the 2005 URSI Conference, Boulder, CO, Jan 5–8, 2005.

[17] Haupt, R. L.
An introduction to genetic algorithms for electromagnetics.
IEEE Antennas and Propagation Magazine, **37** (Apr. 1995), 7–15.

[18] Rappaport, T. S.
Wireless Communications Principles and Practice (2nd ed.).
Upper Saddle River, NJ: Prentice-Hall, 2001.

[19] Lüneburg, R. K.
The Mathematical Theory of Optics.
Berkeley, CA: University of California Press, 1944.

[20] Rondineau, S., Nosich, A. I., Himdi, M., and Daniel, J-P.
Discrete Lüneburg lens fed by a spherical-circular printed antenna in axisymmetrical mode-accurate analysis by MAR.
In *IEEE AP-S Symposium Digest*, San Antonio, TX, June, 2002, 406–409.

[21] Verdú, S.
Multiuser Detection.
London: Cambridge, Aug. 13, 1998.

[22] Kelly, A. and Case, W.
Flying the Earth observing constellations.
Presented at SpaceOps 2004, Montreal, May 2004.

William C. Barott received his B.S., M.S., and Ph.D. in electrical and computer engineering from the Georgia institute of Technology, Atlanta, where he worked on optimization techniques for antennas and arrays.

He is currently an assistant professor in the Electrical and Systems Engineering Department at Embry-Riddle Aeronautical Universtiy in Daytona Beach, FL. His current research activities include radio astronomy, orbit determination, and electric hybrid vehicles.

Mary Ann Ingram received the B.E.E. and Ph.D. degrees in electrical and computer engineering from the Georgia Institute of Technology (Georgia Tech), Atlanta, in 1983 and 1989, respectively.

From 1983 to 1986, she was a research engineer with the Georgia Tech Research Institute, performing studies on radar electronic countermeasure (ECM) systems. In 1986, she became a graduate research assistant with the School of Electrical and Computer Engineering at Georgia Tech where in 1989, she became a faculty member and is currently a professor. In the summers of 2006, 2007, and 2008, she was a visiting professor at the Center for Teleinfrastruktur (CTIF) at Aalborg University in Aalborg, Denmark. Her early research areas were optical communications and radar systems. In 1997, she established the Smart Antenna Research Laboratory (SARL), which emphasizes the application of multiple antennas to wireless communication systems. SARL performs system analysis and design, channel measurement, and prototyping relating to a wide range of wireless applications, including wireless local area network (WLAN), sensor networks and satellite communications, with focus on the lower layers of communication networks.

Dr. Ingram has published over 110 refereed articles, including three that have received "Best Paper" awards at conferences. In fall 2006, she was awarded the ADVANCE Professorship of Engineering. She is a regular reviewer for several conferences, including the IEEE Globecom, IEEE Vehicular Technology Conference (VTC), and Wireless Personal and Mobile Communications (WPMC). She is also a regular reviewer for several IEEE Transactions, including *Communications, Wireless Communications, Antennas and Propagation*, and *Aerospace and Electronic Systems*.

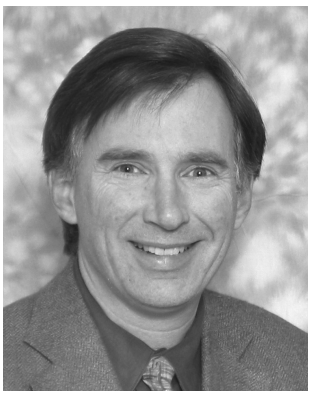

Paul G. Steffes (S'82—M'83—SM'89—F'04) received the S.B. and S.M. degrees in electrical engineering from the Massachusetts Institute of Technology (MIT), Cambridge, MA in 1977, and the Ph.D. degree in electrical engineering from Stanford University, CA, in 1982.

He is a professor and the associate chair for research in the School of Electrical and Computer Engineering at the Georgia Institute of Technology. He joined the faculty of Georgia Tech in 1982. His research program has been supported by NASA, the NSF, the SETI Institute, and a number of industrial sponsors. He has been involved with numerous NASA missions, including Pioneer-Venus, Magellan, the Advanced Communications Technology Satellite (ACTS), the High Resolution Microwave Survey (HRMS) and Juno (Jupiter Polar Orbiter). His research interests include microwave systems for remote sensing of planetary atmospheres and surfaces, spectrum allocations and usage, and microwave communications and navigation systems.

From 1995–2002, Dr. Steffes served on the Committee on Radio Frequencies (CORF) of the National Academy of Sciences, serving as chair from 1998–2001 and past chair from 2001–2002.